Probe Diffusion in Sodium Polystyrene Sulfonate−Water: Experimental Determination of Sphere−Chain Binary Hydrodynamic Interactions

George D. J. Phillies,* Mickey Lacroix, and Jennifer Yambert

Department of Physics, Worcester Polytechnic Institute, Worcester, Massachusetts 01609

Received: February 11, 1997; In Final Form: April 30, 1997[⊗]

Quasi-elastic light-scattering spectroscopy was used to measure the diffusion coefficient of polystyrene latex spheres of diameters 14, 67, and 189 nm in relatively dilute (concentrations $0 \leq c \leq 20$ g/L) solutions of polystyrene sulfonate. Polymer molecular weights were in the range $1.5 \leq M \leq 1188$ kDa; solvents were in the high-salt (0.2M NaCl) regime. The measured low-concentration leading slope dD/dc is compared with the hydrodynamic calculation of this slope obtained from the procedure of Phillies and Kirkitelos (G. D. J. Phillies and P. C. Kirkitelos, *J. Polym. Sci.* **1993**, *31*, 1785), who used a Kirkwood-Risemann (J. G. Kirkwood and J. Riseman, *J. Chem. Phys.* **1948**, *16*, 565) type model for chain hydrodynamics. The experimental and calculated initial slopes agree with each other to within the errors in the experimental measurements.

Introduction

Over the past decade, this laboratory[1] and others[2] have reported extensively on the diffusion of probe spheres through dilute and concentrated polymer solutions. In much of this work, an objective was to use probe diffusion to gain information on chain dynamics, especially in nondilute and semidilute solutions. The dependence of the probe diffusion coefficient on polymer concentration, polymer molecular weight, solution viscosity, and other properties was extensively examined for clues as to the nature of polymer motion at elevated polymer concentrations.

In contrast to this work on polymer diffusion, there is an extensive theoretical[3] and experimental[4] literature on the diffusion of low-concentration (but nondilute) colloidal spheres. At low concentration, pseudovirial expansions for the concentration dependence of D become feasible. The concentration dependence of D can be obtained from ensemble averages over functions of the sphere−sphere hydrodynamic interaction tensors.[5]

Results in this paper represent a hybrid of the above two themes. We studied probe diffusion through a polymer solution. However, the concentration c of the matrix polymer was kept low so that we could extract the initial slope of the concentration dependence of D. If one thinks of D as having a (pseudo)-virial expansion in c, we have determined the second (pseudo)-virial coefficient. This coefficient can also determined by inference from the hydrodynamic model of Phillies and Kirkitelos.[6,7] Just as theoretical calculations[3] of the concentration dependence of D of a sphere in a sphere suspension can be tested experimentally,[4] so also can theoretical calculations[7] of D of a probe in a low-c polymer solution be tested experimentally. Here we report such a set of experiments.

Relative to prior work, the choice of polystyrene sulfonate as the matrix polymer allows us to study probe diffusion in monodisperse matrix polymers having a wide range of molecular weights. Here M_w ranges over more than 3 orders of magnitude, while M_w/M_n is generally below 1.1. We also varied the probe diameter extensively (from 14 to 189 nm), but probe radius turns out not to have a strong effect on the quantities that we determined. At low salt concentration, a variety of peculiar dynamic effects is encountered in polyelectrolyte solutions.[8] The work discussed here was performed using solutions containing 0.2 M NaCl, in which such effects are expected to be substantially absent.

Experimental Methods

Materials. Sodium polystyrene sulfonate (PSS) was from Scientific Polymer Products (molecular weights of 1.5 kDa (M_w = 1540 Da, M_n = 1420 Da), 8.0 kDa (M_w = 7950 Da, M_n = 7200 Da), 38 kDa (M_w = 38.2 kDa, M_n = 28.26 kDa), 178 kDa (M_w = 178 kDa, M_n = 167 kDa), 796 kDa (M_w = 796 kDa, M_n = 691 kDa), and 1.19 MDa (M_w = 1.188 MDa, M_n = 1.126 MDa)) or Pressure Chemical Co. (polymer molecular weight 354 kDa, $M_w/M_n < 1.10$) (all molecular weight data from manufacturers). Surfactants were Triton X-100 (Aldrich, Milwaukee) and sodium dodecyl sulfate (Polysciences, Extra Purified grade, $C_{12} > 99.5\%$). All other materials were reagent grade or higher. Water was 18 MΩ conductivity water from a Millipore Milli-Q water purifier. Polystyrene latex spheres were carboxylate-modified, with nominal diameters of 67 nm (Seradyn), and 14 and 189 nm (Interfacial Dynamics).

Solutions were made by progressive dilution of sphere-containing samples with solvent, starting with a largest PSS concentration of 20 g/L. To guarantee that sphere preparations were stable and did not aggregate during a dilution series, for each polymer molecular weight and sphere diameter we first observed the stability of spheres in a solution of the highest PSS concentration studied. The sphere diffusion coefficient D was determined over a 3 h period, using 15 min integration times at 15 min intervals over a 3 h interval. We required that D did not change significantly during these measurements. Polystyrene spheres in a PSS−0.2M NaCl−H_2O mixture were not adequately stable. Addition of 1 mM NaOH (to ensure that carboxylate residues on the spheres were fully charged) retarded aggregation. Addition of the surfactant Triton X-100 had no further effect on the aggregation process. Joint addition of sodium dodecyl sulfate (SDS) and 1 mM NaOH ended aggregation in most systems, at least for the duration of our experiments. Control experiments established that SDS concentrations as high as 5.2 g/L did not affect D appreciably. We used the minimum SDS concentration that was consistent with sphere stability. This was 0.1 g/L, except for (1) 14 nm spheres in the presence of PSS having $M_w \geq 38$ kDa, for which an

* To whom communications may be addressed. E-Mail: phillies@wpi.wpi.edu.

[⊗] Abstract published in *Advance ACS Abstracts,* June 15, 1997.

S1089-5647(97)00534-8 CCC: $14.00

SDS concentration of 0.32 g/L was required to maintain stability, and (2) 189 nm spheres in 38 or 1188 kDa PSS, which were unstable or did not give reproducible results under any conditions that we investigated.

All dilutions were made with the standard solvent, namely, 1 mM NaOH−0.2M NaCl−0.1 or 0.32 g/L SDS−H_2O; dilutions were determined by weight, using the known density of the solvent and neglecting volume of mixing corrections. Solutions containing polymer and 189 or 67 nm spheres were filtered through 1.2 μm pore diameter cellulosic filters into precleaned scattering cells; solutions containing spheres and 14 nm spheres were instead filtered through 0.22 μm pore diameter filters. Diluents were systematically added by filtering them through 0.22 μm pore diameter cellulosic filters.

Light-scattering spectra were obtained using a 50 mW 533 nm frequency-doubled CW diode laser or a variable-power ($\leq$1.3W) Ar^+ laser. Most experiments were done with a 90° scattering angle. Correlation measurements were made on a Langley-Ford Instruments 144 channel (128 data channels, 16 base line channels) correlator and a Brookhaven Instruments Model 2030 correlator with 270 channels (264 data channels, 6 base line channels). Spectra were very close to exponential, so correlators were consistently operated in their single-tau modes. For polymers with $M_w \geq 178$ kDa, a very weak, very rapid short time decay was barely visible in semilogarithmic plots of probe spectra. Fast, early decays, even if very weak (here, 2−3% of the initial amplitude, for a decay visible only in the first half-dozen correlator channels), delay the convergence of the cumulant expansions used to analyse our spectra. By suppressing data from the first 15 or so correlator channels, we obtained excellent near-single-exponential cumulant fits to our spectra. Physically, we are interpreting the dominant near-single-exponential decay as arising from long-range motion of the probes due to diffusion.

Intensity−intensity time correlation functions $G^{(2)}(t)$ were analyzed by fitting them to a cumulants expansion

$$[G^{(2)}(t) - B]^{1/2} = \sum_{j=0}^{N} \frac{K_j(-t)^j}{j!} \tag{1}$$

Here B is the measured base line, the K_j are cumulants, and N is the truncation level of the fit. The first cumulant K_1 is related to the z-average diffusion coefficient of the probes via $D = K_1/q^2$, where q is the scattering vector. The second-cumulant K_2 gives a measure of the deviation of a spectrum from simple single-exponential behavior. K_2 is usefully expressed as the normalized variance $V = 100\sqrt{K_2}/K_1$. For the 67 and 189 nm spheres, V was independent of polymer concentration; fits with $N = 2$ or sometimes $N = 3$ were adequate to describe spectra to within their underlying signal-to-noise ratios. For the 14 nm spheres, V was generally smaller in polymer-free than in polymer-containing solutions. With 14 nm spheres, V was independent of positive c for all polymer $M \leq 354$ kDa; in 790 kDa PSS, V increased with increasing polymer c.

We also tried fitting spectra to stretched exponentials

$$[G^{(2)}(t) - B]^{1/2} A \exp(-\theta t^{\beta}) \tag{2}$$

where A is the amplitude and θ and β are parameters characterizing the time dependence. The RMS fractional error in a fit to a stretched exponential in time was never better than the fit of the same spectrum to a cumulant series, so throughout the following we used cumulant analyses to interpret $G^{(2)}(t)$.

Under our experimental conditions, scattering by the polystyrene latex spheres substantially dominated scattering by the sodium polystyrene sulfonate−surfactant−salt solutions. A probe-free polymer solution scattered approximately 1% of the light scattered by a corresponding probe-containing polymer solution measured under identical conditions. Control spectra of probe-free polymer solutions were taken under the conditions and integrating times used for our regular measurements. The control spectra were virtually flat to within noise. While there are polymer, surfactant, and small-ion diffusive modes, these modes scatter very little light, so except at larger M they did not contribute appreciably to the measured spectra. At the largest M examined, these modes may have contributed to $G^{(2)}(t)$ at very early times. We eliminated the fast modes by excluding the spectrum at small t from our analyses. Furthermore, the preparation techniques assured that the polystyrene spheres were highly dilute. So long as scattering is dominated by a dilute species, the diffusion coefficient D obtained by quasi-elastic light scattering spectroscopy approximates well the single-particle (self-) diffusion coefficient of that species (here, the polystyrene latex).[9]

Experimental Results

Figures 1−3 show our measurements on probe diffusion through PSS−NaCl−SDS−NaOH−water solutions. In each case D falls with increasing polymer concentration. Lines in the figures represent fits of various simple functions to the data. In summary, for the lower molecular weights (1.5, 8, 38 kDa), a linear dependence

$$D = D_0(1 - ac) \tag{3}$$

on polymer concentration c is adequate. At larger molecular weight, D depends nonlinearly on c. An exponential concentration dependence

$$D = D_0 \exp(-\alpha c) \tag{4}$$

accounts adequately for D, except with the largest-molecular-weight polymer. For probes in solutions of the 1.19 MDa polymer, plots of log D against c do not show straight lines; a stretched-exponential concentration dependence

$$D = D_0 (-\alpha' c^{\nu}) \tag{5}$$

fits D well. In the above, D_0 is the low-concentration limiting value for D, while a, α, and α' describe the low-c concentration dependence of D, and ν is a stretching exponent.

Figure 1 shows D for all probe sizes and the 1.5, 8, 38, and 178 kDa PSS. Solid lines are fits to eq 3; fitting parameters appear in Table 1. For spheres in 178 kDa PSS (Figure 1d), D is clearly not linear in c over the full concentration range studied. For the 178 kDa PSS, the leading slope for D against c was estimated by fitting eq 3 to D for $0 < c \leq 10$ g/L. Despite our precautions, D for 14 nm spheres in 1.5 kDa PSS and for 67 nm spheres in 8 kDa PSS were considerably more scattered than D for other sphere−polymer combinations; we did not include results from these sphere−polymer combinations in our further analysis.

Figure 2 shows D for all probes in solutions of the 178, 354, 796, and 1188 kDa PSS. Solid lines are fits to simple exponentials (eq 4). Parameters appear in Table 1. Exponentials were also fit to D of probes in solutions of the 1.5, 8, and 38 kDa PSS. Those resulting exponentials were very close to the straight lines seen in Figure 1a,c. For spheres in solutions of 1188 kDa PSS, a simple exponential does not describe D at elevated concentrations. Our interest here is the leading slope of D against c. For spheres with 1188 kDa PSS, this slope

was obtained by fitting D for the lower-c region $0 \le c \le 12$ g/L to eq 4, as reported in Figure 2d and Table 1.

Figure 3 presents stretched-exponential fits to D of spheres in the 790 kDa and 1.19 MDa PSS solutions. Parameters for these curves appear in Table 2. For both polymer molecular weights and all three sphere diameters, stretched-exponential forms account well for the concentration dependence of D of each sphere−polymer combination, out to the largest concentrations studied.

Theoretical Analysis

The self-diffusion coefficient of a particle is related[3] to its mobility tensor μ_{ij} via

$$D = k_B T \langle \mu_{ii} \rangle \tag{6}$$

where k_B is Boltzmann's constant, T is the absolute temperature, and the self part μ_{ii} of the mobility tensor is a function of particle coordinates, necessitating the indicated ensemble average $\langle \cdots \rangle$. The mobility tensors connect the total nonhydrodynamic forces $\mathbf{F}_j$ on particles j to the induced velocity $\mathbf{v}_i$ of a particle i, namely

$$\mathbf{v}_i = \sum_{j=1}^{N} \mu_{ij} \cdot \mathbf{F}_j \tag{7}$$

The self and distinct parts of μ_{ij} may be written[5]

$$\mu_{ii} = \frac{1}{f_o}(\mathbf{I} + \sum_{l \neq i=1}^{N} b_{il} + \cdots) \tag{8}$$

and

$$\mu_{ij} \frac{1}{f_o}(T_{ij} + \sum_{l \neq (i,j)=1}^{N} T_{ilj} + \cdots) \tag{9}$$

respectively. Here f_o is the bare drag coefficent of particle i and $\mathbf{I}$ is the identity tensor.

The derivations of Mazur and van Saarloos[5] lead to explicit forms for the $\mathbf{T}$ and b tensors. The derivations assume that the fluid is incompressible and Newtonian, that inertial effects can be neglected, and that the interacting objects are nonoverlapping spheres that provide stick boundary conditions and exclude solvent flow from their interiors. The lead terms of the $\mathbf{T}$ and $\mathbf{b}$ tensors are[5]

$$T_{ij} = \frac{3}{4}\frac{a_i}{r_{ij}}(\mathbf{I} + \hat{r}_{ij}\hat{r}_{ij}) + \frac{1}{4}\frac{a_i}{r_{ij}}\frac{(a_i^2 + a_j^2)}{r_{ij}^2}(\mathbf{I} - 3\hat{r}_{ij}\hat{r}_{ij}) \tag{10}$$

and

$$b_{il} = -\frac{15}{4}\left(\frac{a_i a_l^3}{r_{il}^4}\right)\hat{r}_{il}\hat{r}_{il} + \cdots \tag{11}$$

In the above, a_i is the radius of sphere i, $\hat{r}_{ij}$ is the unit vector pointing from particle i toward particle j, $\hat{r}_{ij}\hat{r}_{ij}$ is a dyadic product, and r_{ij} is the distance between particles i and j.

This hydrodynamic approach can also be used to compute b_{il} and T_{ij} for a pair of polymer chains, as was done by this author and Kirkitelos.[6,7] These calculations used the Kirkwood−Risemann model[10] for a polymer chain, in which a chain having radius of gyration R_g and hydrodynamic radius R_h is represented as a sequence of N linked beads, each bead having a hydrodynamic radius a. Hydrodynamic interactions between pairs of beads were modeled with eqs 10 and 11 and their higher-order (in a/r) expansions; the analysis in this paper refers to a truncation of the bead−bead interaction T_{il} at the level of the Rotne−Prager ($O((a/r)^3)$) approximation. The calculation of refs 6 and 7 was based on the method of reflections, hydrodynamic interactions being propagated via eq 10, with $a_i = a_j$ being applied as a simplification. Whole-chain motions entered via the requirements that the total force and torque on each chain must vanish.

The hydrodynamic approach of refs 6 and 7 can be used to calculate how the diffusion of a single large sphere is modified,

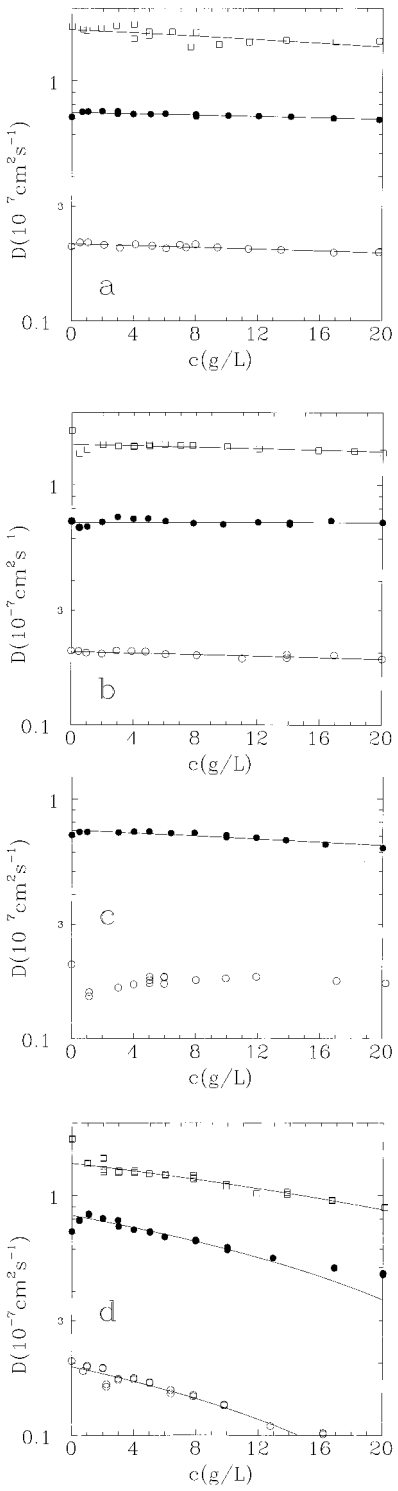

Figure 1. Diffusion coefficient of 14 nm (squares), 67 nm (filled circles), and 189 nm (open circles) polystyrene latex spheres in PSS−NaCl−NaOH−SDS. PSS molecular weights were (a) 1.5, (b) 8, (c) 38, and (d) 178 kDa (c < 11 g/L data only). Lines represent best-fit linear concentration dependences, with outlier points excluded.

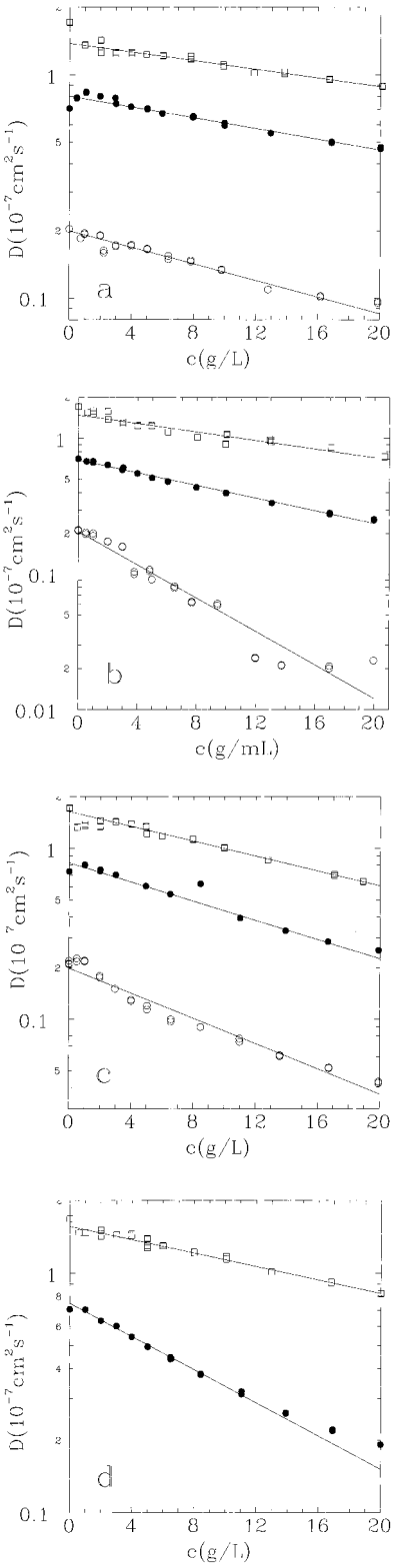

Figure 2. Diffusion coefficient of 14 nm (squares), 67 nm (filled circles), and 189 nm (open circles) polystyrene latex spheres in PSS−NaCl−NaOH−SDS. PSS molecular weights were (a) 178, (b) 354, (c) 790, and (d) 1188 kDa. Lines represent best-fit simple-exponential concentration dependences, with outlier points excluded. For d, $0 < c < 12$ points were fit.

to lowest order in concentration, by the presence of a surrounding matrix of dilute chains. In fact, the calculation in ref 7 treating two polymer chains has done almost all the necessary work, if one applies the special conditions that (1) the probe chain contains only a single monomer, but (2) the monomer has the radius of a polystyrene sphere probe. Specifically, on

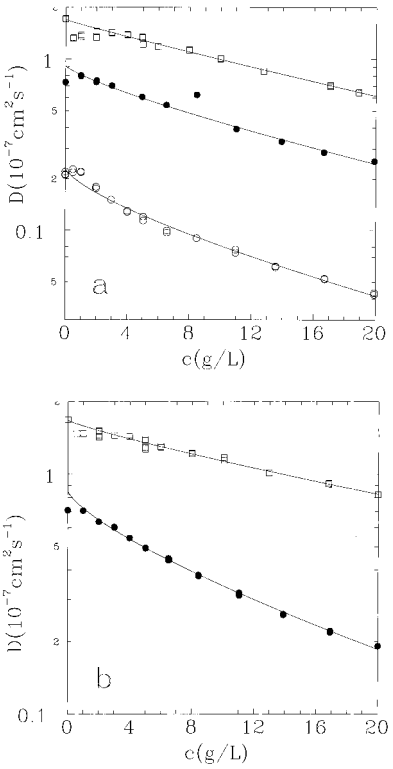

Figure 3. Diffusion coefficient of 14 nm (squares), 67 nm (filled circles), and 189 nm (open circles) polystyrene latex spheres in (a) 790 kDa and (b) 1.19 MDa PSS−NaCl−NaOH−SDS. Lines represent best-fit stretched-exponential concentration dependences, with outlier points excluded.

requiring in each step in ref 7's calculation (their eqs 47−62) that each factor of a, R_h, and R_g is correctly associated with the first or second chain and that a_i and a_j are retained as distinct variables in eq 10, one finds that the self part of the chain−chain hydrodynamic interaction tensor b becomes[7]

$$b_{il}^{(ch,ch)} = -\frac{9}{8}\frac{R_{hi}R_{hl}R_{gl}^2}{r_{il}^4}\hat{r}_{il}\hat{r}_{il} + \frac{9}{4}\frac{R_{hi}R_{hl}R_{gl}^2(a_i^2 + a_l^2)}{r_{il}^6}\hat{r}_{il}\hat{r}_{il} - \frac{3}{8}\frac{R_{hi}R_{hl}R_{gl}^2(a_i^2 + a_l^2)^2}{r_{il}^8}(\mathbf{I} + 2\hat{r}_{il}\hat{r}_{il}) \quad (12)$$

Here i and l label chains, R_{hi} and R_{hl} are the hydrodynamic radii of the two chains, R_{gl} is the radius of gyration of the second chain, a is the bead radius, and r_{il} and $\hat{r}_{il}$ are now the interchain distance and interchain direction unit vector.

In deriving eq 12, ref 7 writes the distance between a pair of beads, one in each chain, as $-\mathbf{s}_i + \mathbf{r}_{il} + \mathbf{s}_l$, where $\mathbf{r}_{il}$ is the vector between chain center of masses and where $\mathbf{s}_i$ and $\mathbf{s}_l$ are vectors from the chain centers of mass to their respective beads. Reference 7 then does a series expansion in $|\mathbf{s}_i|$ and $|\mathbf{s}_l|$, retaining terms of zeroth order in $|\mathbf{s}_i|$ and up to second order in $|\mathbf{s}_l|$. The differences in numerical factors between eqs 12 and 11 arise because the body l was treated as a cloud of beads in the latter calculation, but as a single sphere in the former calculation. In both calculations, the body i was effectively treated as a hydrodynamic point. Equation 12 therefore remains correct—to its current order of approximation—if i is taken to be a single sphere of radius $R_{hi} = a_i$, as opposed to being a cloud of polymer beads having hydrodynamic radius R_h.

To compute D from eq 6, one takes an average of μ_{ii} and hence (via eq 8) $b_{il}^{(ch,ch)}$ over an ensemble of l chains, as seen in

TABLE 1: Diffusion of 189, 67, and 14 nm Spheres through Polystyrene Sulfonate: 0.2 M NaOH−1.0 mM NaCl−0.1−0.32 g/L SDS [See Text]

		$D = D_0(1 - ac)$			$D = D_0 \exp(-\alpha c)$		
M (kDa) [c^*][a] (g/L)	R(nm)	D_0	a	%RMSE[b]	D_0	α	%RMSE
1.5	189	0.21	4.1×10^{-3}	1.6	0.21	4.3×10^{-3}	1.6
[73]	67	0.74	3.2×10^{-3}	1.4	0.74	3.3×10^{-3}	1.4
	14	(1.64)[c]	(7.7×10^{-3})	4.8	(1.63)	(8.5×10^{-3})	4.7
8.0	189	0.20	3.5×10^{-3}	1.5	0.20	3.6×10^{-3}	1.5
[32]	67	(0.70)	(0)	2.6	(0.72)	(3.5×10^{-3})	3.5
	14	1.47	4.4×10^{-3}	3.9	1.47	3.2×10^{-3}	1.6
38	67	0.74	6.8×10^{-3}	2.0	0.74	7.2×10^{-3}	2.1
[14]	14	1.67	8.6×10^{-3}	2.5	1.67	9.6×10^{-3}	1.5
178	189	0.19	3.3×10^{-2}	4.5	0.19	4.3×10^{-2}	3
[6.7]	67	0.79	2.8×10^{-2}	2.4	0.81	2.7×10^{-2}	1.3
	14	1.36	1.8×10^{-2}	3.3	1.38	2.2×10^{-2}	3.0
354	189	nuf[d]	nuf[d]	nuf[d]	(0.21)	(0.14)	10
[4.7]	67	nuf[d]	nuf[d]	nuf[d]	0.69	5.3×10^{-2}	3
	14	nuf[d]	nuf[d]	nuf[d]	1.48	(3.6×10^{-2})	6.9
796	189	nuf[d]	nuf[d]	nuf[d]	(0.20)	(8.5×10^{-2})	10
[3.2]	67	nuf[d]	nuf[d]	nuf[d]	0.82	6.5×10^{-2}	4
	14	nuf[d]	nuf[d]	nuf[d]	1.63	5.0×10^{-2}	3
1188	67	nuf[d]	nuf[d]	nuf[d]	0.75	8×10^{-2}	1.6
[2.6]	14	nuf[d]	nuf[d]	nuf[d]	1.56	3.2×10^{-2}	3

[a] Here $c^* = 3M/(4\pi R_g^3 N_A)$ is the overlap concentration, based on $R_g(M)$ from ref 11. [b] %RMSE = root-mean-square fractional error (%) in each fit. [c] Parenthesized parameters denote unsatisfactory fits not used in further analyses. [d] nuf = no useful fit.

TABLE 2: Diffusion of 189, 67, and 14 nm Spheres through Polystyrene Sulfonate: 0.2 M NaOH−1.0 mM NaCl−0.1−0.32 g/L SDS [See Text] and Fits to $D = D_0 \exp(-\alpha' c^\nu)$

M (kDa)	R(nm)	D_0	α′	ν	%RMSE[a]
796	189	0.23	0.20	0.72	6.4
	67	0.92	0.12	0.80	2
	14	1.70	6.3×10^{-2}	0.93	4
1190	67	0.85	0.166	0.74	1.7
	14	1.67	5.5×10^{-2}	0.85	2.2

[a] %RMSE = root-mean-square fractional error (%).

ref 7, eqs 38−42. Repeating this calculation while noting that the distance of closest approach of two beads is now $a_i + a_l$ rather than $2a$, and averaging eq 12, one obtains

$$D = D_o\left(1 + n\left[\left(\frac{4\pi R_{hi} R_{hl} R_{gl}^2}{(a_i + a_l)}\right)\left(-\frac{3}{8} + \frac{1}{4}\frac{(a_i^2 + a_l^2)}{(a_i + a_l)^2} - \frac{1}{8}\frac{(a_i^2 + a_l^2)^2}{(a_i + a_l)^4}\right)\right]\right) \quad (13)$$

D_o is the diffusion coefficient of an i particle in pure solvent, while n is the number density of l chains. On converting n to a mass concentration via $c = n\,M/N_A$, N_A being Avogadro's number, one has $D = D_o(1 - \alpha_t c)$. The computed leading slope α_t at the level of approximation of the calculation of Phillies and Kirkitelos[7] for a sphere of radius a_i diffusing through a polymer solution is therefore

$$\alpha_t = \frac{N_A}{M}\left[\left(\frac{4\pi R_{hi} R_{hl} R_{gl}^2}{(a_i + a_l)}\right)\left(-\frac{3}{8} + \frac{1}{4}\frac{(a_i^2 + a_l^2)}{(a_i + a_l)^2} - \frac{1}{8}\frac{(a_i^2 + a_l^2)^2}{(a_i + a_l)^4}\right)\right] \quad (14)$$

So long as $a_i \gg a_l$, as is the case here in that probe radii are ≥7 nm while bead radii are ≤0.5 nm, α_t is very nearly independent of a_l.

Related Considerations

Equation 14 for α_t depends on the sphere radius a_i and a variety of parameters describing the polymer chains, notably their hydrodynamic radius R_{hl}, radius of gyration R_{gl}, and bead radius a_l. R_h and R_g for polystyrene sulfonates were extensively studied by Peitzsch, et al.[11] who used static and dynamic light scattering to obtain these parameters for polystyrene sulfonate and several other polymers, at ionic strengths from 10 mM to 1 M and a series of concentrations below 15 g/L, for polystyrene sulfonate molecular weights of 35, 74, 200, 780, and 1200 kDa. Peitzsch et al. found that D and hence R_h scale accurately with $M^{0.5}$ and have a linear dependence on $c_s^{1/2}$, c_s being the salt concentration. These are the data required here for a quantitative evaluation of eq 14.

Before using Pietzsch et al.'s data,[11] it seems necessary to remark upon a seeming peculiarity in their measurements—of which they were aware—namely that, for 780 kDa PSS in 2, 15, and 4000 mM NaCl, R_g increases by more than 2.5 fold with decreasing ionic strength, but R_h increases by no more than 50% over the same range of salt concentrations. These results are not altogether expected, because they imply that R_g and R_h are independent quantities, contrary to theoretical expectations discussed in ref 11. Pietzsch et al. noted a similar effect for several other polyelectrolytes that they studied. If one can give a rational physical explanation for this phenomenon, then it appears safe to use the data; on the other hand, if the observed behavior is physically unreasonable, one is obliged to worry if an unidentified artifact has created errors in the measurements.

We may readily propound a physical interpretation for the observations. Suppose a polymer chain is envisioned as a cloud of beads whose density falls off with distance from the chain center of mass. Near the chain center, the bead density is high, so solvent is entrained and moves with the chain. Further out from the center, the density of polymer beads is lower, so the solvent is free to move with respect to the chain. Let d be the average distance from the center of mass at which draining behavior replaces non-draining behavior; d corresponds to the hydrodynamic radius. (One does not expect $d = R_h$, because beads outside d also contribute to hydrodynamic drag.) Some beads are located within d of the center of mass. These beads are embedded in a mass of entrained solvent, rather than moving with respect to the local solvent motions, so the contribution of these beads to R_h is not dependent on their precise positions. Moving these beads changes R_g but not R_h.

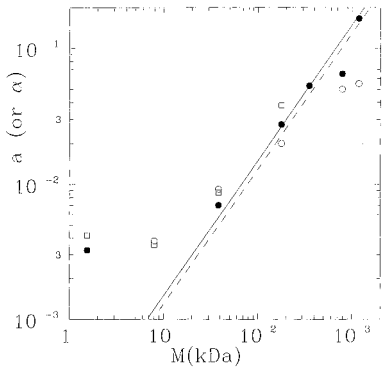

Figure 4. Initial slope for 14 nm (open circles), 67 nm (filled circles), and 189 nm (squares) spheres against polymer molecular weight M. Lines represent (solid) the theoretical value for a and (dashed) the best fit for M above 10 kDa to $a = a_0 M^1$.

Consider a polyelectrolyte. How will R_g and R_h depend on the ionic strength I ? Reducing I increases repulsions between nearby beads, making it more likely that beads will be found further apart and selectively reducing the bead density in the densest parts of the chain—the parts nearest the chain center. Unless beads moving out from the center are moved beyond d, reducing I will increase R_g without increasing R_h to nearly the same extent, consistent with the observations of Pietzsch et al.[11] A quantitative confirmation of this interpretation awaits computer simulations, but the qualitative observations of Pietzsch et al. are physically plausible.

For 780 kDa PSS, Pietzsch et al.[11] find for the radius of gyration $\langle R_g^2 \rangle = 1.01 \times 10^5 + 1.45 \times 10^6 c_s^{-0.5}$, c_s being the ionic strength in mM and S being in angstroms. Here $c_s = 200$, so $R_g \approx 460$ Å. Interpolating on Figure 8a of ref 11, one finds $R_h \approx 230$ Å for the same polymer.

Equation 14 for α_t also depends on the probe radius a_i and on the bead radius a_l. a_i may be determined from the diffusion coefficient of the probes in pure water; for our probes, a_l is approximately 7, 33, or 95 nm for our probes. So long as $a_i \gg a_l$, as is the case here, an accurate a_i is not important: the first of the parenthesized terms in eq 14 is $\approx a_i$, while other terms depend on a_i and a_l approximately as $(a_l/a_i)^N \approx 1$. In refs 6 and 7, a_l is the physical diameter of a polymer chain, not a renormalizable free parameter, but details of the solvent−polymer interaction leave a_l less accurately known than the other radii are known. Fortunately, α_t is nearly independent of a_l, so even a substantial error in estimating a_l has little effect on α_t. We used $a_l \approx 3.5$ Å for the chain thickness. On combining these auxiliary data with eq 14, one can compute α_t.

Analysis

As discussed above, several slightly different functional forms were used here to determine the initial slope, the different forms giving fits of similar quality and modestly different initial slopes. For probes in the 1.5, 8, 38, and 178 kDa PSS, the linear- and simple- exponential fits are approximately equally acceptable, so for further analysis, the initial slope for each polymer and probe was taken to be the average of the two fits. For probes in the 354 and 796 kDa PSS, the simple exponential fit is entirely adequate, so α is used for the initial slope. For probes in 1.19 MDa PSS, α' is taken from the fit to the stretched exponential.

Figure 4 shows our best experimental estimates of a and α for all sphere radii and polymer molecular weights. Below 10 kDa, a is nearly independent of polymer M. At large M, a and α increase dramatically with increasing M, ranging from $\approx 3 \times 10^{-3}$ at $M \approx 10$ kDa to ≈ 0.17 at $M \approx 1.2$ MDa.

The solid line in Figure 4 indicates the theoretical value of α_t, based on eq 14 and polymer and probe properties and molecular weight dependences given in the previous section. α_t was computed numerically for 67 nm spheres and 780 kDa PSS and extrapolated to other molecular weights with the molecular weight dependence $\alpha_t \sim M^1$ implied by Pietzsch et al.'s[11] finding that the chain radius of PSS scales as $M^{1/2}$. α_t depends so weakly on probe radius that α_t curves for different chain radii are scarcely different on the scale of the figure. It should be emphasized that there are no free parameters available to adjust the position of the solid line relative to the measurements.

The dashed line is a least-mean-squares fit of the experimental data for $M > 10$ kDa to $a = a_0 M^1$, a_0 being the free parameter. The quantity being minimized was the fractional RMS error

$$R = \sum_{i=1}^{N} \frac{(D_i - T_i)^2}{D_i T_i} \tag{15}$$

where D_i and T_i are the measured and theoretical values of a for the i^{th} of the N data points. For a nominal 1 MDa polymer, the best-fit line gives $a = 0.128$ (for c in g/L). For probes in solutions of a 1 MDa PSS, results of the two previous sections give theoretical estimates α_t of 0.145, 0.150, or 0.151 for the 14, 67, and 189 nm spheres, respectively. The theoretical and best-fit lines are indeed extremely close, differing by less than 20% at any M.

Discussion

Here we have used quasi-elastic light-scattering spectroscopy to measure the diffusion of spherical probe particles through solutions of sodium polystyrene sulfonate in NaCl solution. Our primary concern was to determine the initial slope $a = \lim_{c\to 0} dD/dc$ of the concentration dependence of D. Determining this slope became increasingly difficult as polymer M became larger. Relative to many of our other studies[1] of probe diffusion in polymer solutions, the polymers studied here are relatively dilute ($c \leq 20$ g/L) and highly monodisperse ($M_w/M_n \lesssim 1.1$).

Our experimental values for a were compared with the hydrodynamic polymer model of Phillies and Kirkitelos.[7] For our purposes, it was necessary to specialize the calculation in ref 7 to the case in which the probe "polymer" chain contained a single, large monomer bead, leading to eq 14 for the theoretical slope α_t.

From Figure 4, for $M > 10$ kDa the calculated α_t is in good agreement with experiment, the difference between the theoretical and best-fit lines being much smaller than the visible scatter in the data. We conclude that our measurements provide direct experimental confirmation of the approximate accuracy of the Phillies−Kirkitelos[7] procedure for calculating the self-component b_{il} of the chain−chain hydrodynamic interaction tensor. Phillies and Kirkitelos extended their calculation of b_{il} to higher concentrations via a self-similarity assumption. Our measurements speak only to the accuracy of their low-concentration (two-chain) calculation. The analysis given here is not a test of self-similarity.

At lower molecular weights, the model calculation of α_t does not work well. At these low molecular weights, it is probably not realistic to model the PSS chains as spherical clouds of frictional points. A rod model would be more appropriate than the hydrodynamic model of ref 7.

A physical quantity analogous to a also arises in the theory of self-diffusion by hard spheres, for which the standard prediction[3] is $D = D_o(1 - a'\phi)$ with $a' = 1.73$ for ϕ the sphere volume fraction. If one converted this prediction from volume fraction to the concentration (g/L) units used here, one would have $a' \approx 0.001$ for organic spheres independent of sphere molecular weight. a' and a can be dramatically different, especially at large M where $a/a' \geq 100$. This difference is found because polymer coils are highly open objects; the volume within R_h of the center of a polymer chain typically contains far more solvent than polymer. As a result of their openness, the effective hydrodynamic volume of a polymer coil is far larger than the physical volume of the polymer molecule itself, so polymer coils are far more effective than equal masses of solid spheres at retarding the motion of probe spheres.

Acknowledgment. The partial support of this work by the National Science Foundation under Grant DMR94-23702 is gratefully acknowledged.

References and Notes

(1) (a) Ullmann, G.; Phillies, G. D. J. *Macromolecules* **1983**, *16*, 1947. (b) Lin, T.-H.; Phillies, G. D. J. *Macromolecules* **1984**, *17*, 1686. (c) Phillies, G. D. J.; Quinlan, C. A. *Macromolecules* **1992**, *25*, 3310.

(2) (a) Mustafa, M. B.; Russo, P. S. *J. Colloid Interface Sci.* **1989**, *129*, 240. (b) Yang, T.; Jamieson, A. M. *J. Colloid Interface Sci.* **1988**, *126*, 220. (c) Brown, W.; Rymden, R. *Macromolecules* **1986**, *19*, 2942.

(3) Beenakker, C. W. J.; Mazur, P. *Phys. Lett.* **1982**, *91*, 290.

(4) (a) Mos, H. J.; Pathmamanoharan, C.; Dhont, J. K. G.; deKruif, C. G. *J. Chem. Phys.* **1985**, *84*, 45. (b) Kops-Werkhofen, M.-M.; Vrij, A.; Lekkerkerker, H. N. W. *J. Chem. Phys.* **1983**, *78*, 2760. (c) Qiu, X.; Wu, X. L.; Xue, J. Z.; Pine, D. J.; Weitz, D. A.; Chaikin, P. M. *Phys. Rev. Lett.* **1990**, *65*, 516.

(5) Mazur, P.; van Saarloos, W. *Physica A* **1982**, *115*, 1.

(6) Phillies, G. D. J. *Macromolecules* **1988**, *21*, 3101.

(7) Phillies, G. D. J.; Kirkitelos, P. C. *J. Polym. Sci.* **1993**, *31*, 1785.

(8) Schmitz, K. S. *An Introduction to Dynamic Light Scattering by Macromolecules*; Academic Press: Boston, 1990; Chapter 10.

(9) Phillies, G. D. J. *J. Phys. Chem.* **1995**, *99*, 4265.

(10) Kirkwood, J. G.; Riseman, J. *J. Chem. Phys.* **1948**, *16*, 565.

(11) Peitzsch, R. M.; Burt, M. J.; Reed, W. F. *Macromolecules* **1992**, *25*, 806.